Monitoring of molecule adsorption and molecular wire formation by in situ surface plasmon resonance spectroscopy

Rodica Morarescu, Frank Träger, and Frank Hubenthal

***Abstract*—We have investigated adsorption of different molecules and molecular wire formation on gold nanoparticles by in situ surface plasmon resonance spectroscopy. For this purpose, highly ordered gold nanoparticle arrays on fused silica have been prepared by nanosphere lithography and served as plasmonic substrates. Two arrays with different sized triangular nanoparticles, either with a base of the triangle of (74 ± 6) nm or with a base of the triangle of (465 ± 28) nm, were used for the sensitivity measurements. After molecular adsorption on the nanoparticles, we observed significantly larger plasmon shifts and an up to 4 times higher sensitivity for the small triangular nanoparticles. This higher sensitivity is attributed to their higher surface to volume ratio compared to the large triangular nanoparticles. After the sensitivity measurements, molecular wire formation has been performed using a ruthenium complex, a double cyclodextrin unit, and an iridium complex. The molecules have been stepwise assembled on highly ordered small triangular gold nanoparticles, which served as anchor points. We observed distinct shifts of the plasmon resonance from 20 nm to 46 nm, depending on the wire length. The results demonstrate that a molecular wire formation can be monitored with high sensitivity and in situ by surface plasmon resonance spectroscopy.**

***Index Terms*—Gold nanoparticles, Nanosphere lithography, Plasmon resonance spectroscopy, Triangular nanoparticles**

I. Introduction

In recent years, fundamental and applied research on nanostructures has been steadily increased. The reason is the high potential of nanostructures for a broad variety of applications [1–13]. One particular nanostructure that exhibits extraordinary optical properties are metal nanoparticles. Since centuries the magnificent colors of stained glass, for example in old church windows [14] or drinking cups, such as the Lycurgos cup [15], have attracted great attention. However, the origin of the colors remaind unknown for a long time. The first one, who referred the colors to metal nanoparticles, was Michael Faraday. In his famous article entitled *Experimental Relations of Gold (and Other Metals) to Light* from 1857 he concluded [16]: *I think that in all these cases the ruby tint is due simply to the presence of diffused finely-divided gold.* The first theoretical explanation of the colors came up approximately fifty years later in 1908 by Gustav Mie. He applied the Maxwell equations in spherical coordinates to small spheres in homogeneous environments [17] to explain the experimental findings of his students [18]. With this pioneering work, he could trace the origin of the colors back to a resonant absorption of light by small metal spheres. This resonant absorption, which is caused by a collective excitation of conduction band electrons in metal nanoparticles, is nowadays called localized surface plasmon polariton resonance. For simplicity, we refer to this kind of excitation as surface plasmon or simply plasmon.

A variety of alkaline and noble metals exhibit pronounced plasmon resonances. But due to their great potential for applications, gold nanoparticles have been widely investigated in recent years [1, 3–5, 19–28]. The reason is their extraordinary and tuneable optical properties. The position of the plasmon resonance can easily be tuned over a wide spectral range by varying nanoparticle size, shape, composition, and dielectric surrounding [23, 26, 29–37]. Furthermore, the excitation of surface plasmons is accompanied by a local field enhancement, which is exploited in many extremely different applications, such as surface-enhanced Raman spectroscopy [1, 2, 38–44], wave guiding [45, 46], surface-enhanced fluorescence [47–49], and confocal microscopy [50], as well as to enhance the efficiency of solar cells [10], or to structure surfaces [8, 9, 11, 12, 51, 52].

For plenty applications, regular arrays of metal nanoparticles are desired. They may serve, for example, as anchor points for electro-optic active molecules, used for electro-optical devices. Usually, metal nanoparticle arrays are prepared by electron beam lithography [53–55] or photolithography [56, 57]. While electron beam lithography is time consuming and expensive, photolithography has lower limits concerning nanoparticle size. To overcome the aforementioned drawbacks, nanosphere lithography (NSL) [58] can be used. NSL is an inexpensive technique to prepare regular arrays of highly ordered triangular nanoparticles [55, 59–62] with a high throughput. The size of the generated nanoparticles can easily be varied by changing the amount of deposited material and/or the diameter of the nanospheres used as a mask. The nanoparticle shape and size as well as the distance between to particles can be changed by variation of the nanosphere mask [63], tilt evaporation [62] or laser tailoring [59, 64].

In this paper, we present recent measurements with the objective to monitor a molecular wire formation by in situ

Manuscript received March 23, 2011.

Rodica Morarescu, Université de Mons Laboratoire Interfaces &, Fluides Complexes, Centre d' Innovation et de Recherche en Matériaux, Polymères, 20 Place du Parc, 7000 Mons, Belgium.

Frank Träger, University of Kassel, Institute of Physics, and CINSaT, Heinrich-Plett-Str. 40, 34132 Kassel.

Frank Hubenthal, University of Kassel, Institute of Physics, and CINSaT, Heinrich-Plett-Str. 40, 34132 Kassel.

Manuscript received April 19, 2005; revised January 11, 2007.

surface plasmon resonance spectroscopy. For this purpose, highly ordered triangular gold nanoparticles on substrates have been prepared by NSL. The advantage of using triangular gold nanoparticles for surface plasmon resonance spectroscopy is their high surface to volume ratio, which yields higher sensitivity compared to, for example, spherical nanoparticles of same size. We demonstrate that we can monitor clearly distinct and stepwise shifts of the plasmon resonance due to subsequent attachment of different molecules, which form a wire. In addition, elongated nanoparticles have been prepared by NSL for confocal microscopy measurements.

II. Experimental

Arrays of small and large triangular as well as large elongated gold nanoparticles were prepared using nanosphere lithography, utilizing the drop coating method of Micheletto et al. [65]. Quadratic fused silica plates with an edge length of 12 mm and a thickness of 5 mm served as substrates. Different lithographic masks have been prepared using monodisperse latex nanospheres, either with a diameter of 330 nm or of 1390 nm. After formation of large areas of well ordered monolayers or doublelayers of nanospheres on a substrate, the sample were transferred to a thermal evaporation chamber (Balzers BA 510). At a pressure of approximately 10^{-6} Pa, a gold film has been prepared on the sample. For the small triangles the gold film thickness was set to 30 nm, while for the large triangular and elongated nanoparticles, the gold film thickness was set to 150 nm. After film deposition, the nanosphere mask was removed by sonicating the sample for 1 to 3 minutes in dichloromethane, leaving behind large areas of highly ordered gold nanoparticles, as depicted in figure 1. Depending on the number of nanosphere layers, triangular nanoparticle (monolayer mask) or elongated nanoparticles (double layer mask) have been generated. Details of the preparation have been explained in reference [66].

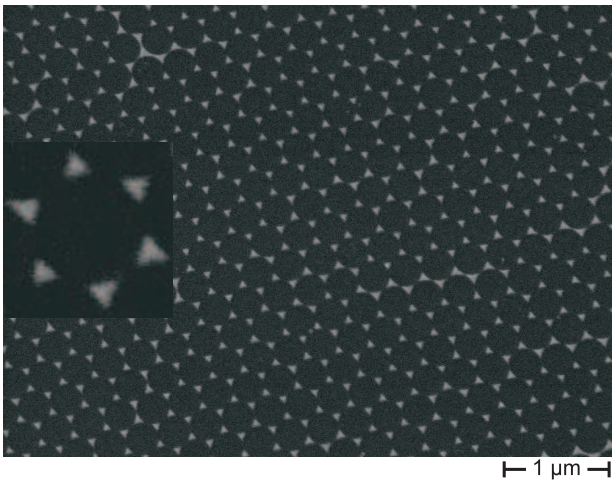

Fig. 1. Large area SEM image of small triangular nanoparticles generated by NSL. The inset shows a magnification, demonstrating their triangular shape. Depicted are nanoparticles with a side length of (74 ± 6) nm and a height of (30 ± 4) nm.

To characterize the samples optical spectroscopy, scanning electron microscopy (SEM), and atomic force microscopy (AFM) were applied. While optical spectroscopy has been performed mainly to measure plasmon shifts, microscopy techniques have been solely applied to determine the morphology of the nanoparticles.

For the sensitivity measurements small and large triangular gold nanoparticles have been applied, generated either by monolayers of 330 nm or 1390 nm nanospheres as lithographic mask. However, only small triangular nanoparticles have been used for monitoring wire formation by in situ surface plasmon resonance spectroscopy.

To demonstrate that the molecules attach selectively to the nanoparticles and not to the substrate, confocal microscopy has been applied. Due to the limited optical resolution of the confocal microscope, large elongated nanoparticles have been used for the fluorescence measurements. To generate the large elongated nanoparticles a doublelayer mask of 1390 nm nanospheres has been prepared on part of the substrate, whose other part is covered with a monolayer mask. Since tilt coating has been used to prepare the doublelayer masks, the second nanosphere layer was slightly shifted with respect to the first layer. As a result, besides the large triangular nanoparticles, elongated nanoparticles with an average side length of (365 $\pm$ 16) nm, a height of (150 $\pm$ 10) nm and a particle-particle distance of about (1484 $\pm$ 20) nm were generated.

For the sensitivity measurements and the wire formation five different recently synthesized molecules have been used, which yield high potential for future applications in molecular electronic devices. The first two molecules, a ruthenium complex (ruthenium complex **1**) ([Ru(bpy)(bpySH)]$(PF_6)_2$) and an europium complex EuSH have been solely used for sensitivity measurements. While a second ruthenium complex (ruthenium complex **2**) ([Ru(biptpy)(tpySS)]$(NO_3)_2$) has been used for sensitivity measurements and as anchor molecule for wire formation. Molecule four consists of two connected cyclodextrins (bis-propargyl-p.m.-CD) and serves as a connecting molecule between the ruthenium complex **2** and the fifth molecule, which is an iridium complex ([Ir(bibtpy)(tpy)]$(PF_6)_3$). The chemical structure of the molecules is depicted in figure 2.

For the sensitivity measurements, the europium and both ruthenium complexes have been adsorbed on small and large triangular gold nanoparticles. For this purpose, the samples with the nanoparticle arrays have been immersed for 24 hours in a 1 mM solution of the respective molecule. Subsequently, the samples were washed with the solvent used for the molecule solution and dried in a gentle stream of nitrogen. Finally, an extinction spectrum has been recorded.

Wire formation has been performed as follows. The attachment of the anchor molecule has been achieved by immersion of a sample with small gold nanoparticles for 24 hours in a methanolic solution (1 mM) of the ruthenium complex **2**. Thereafter, the sample was washed with methanol in order to remove any excess of the ruthenium complex **2**. Afterwards, the sample was dried with a gentle flow of nitrogen and an extinction spectrum has been recorded. In addition, confocal microscopy images of the sample have been recorded after adsorption of the ruthenium complex **2**. To complete the wire, the sample with the ruthenium complex **2** has been immersed

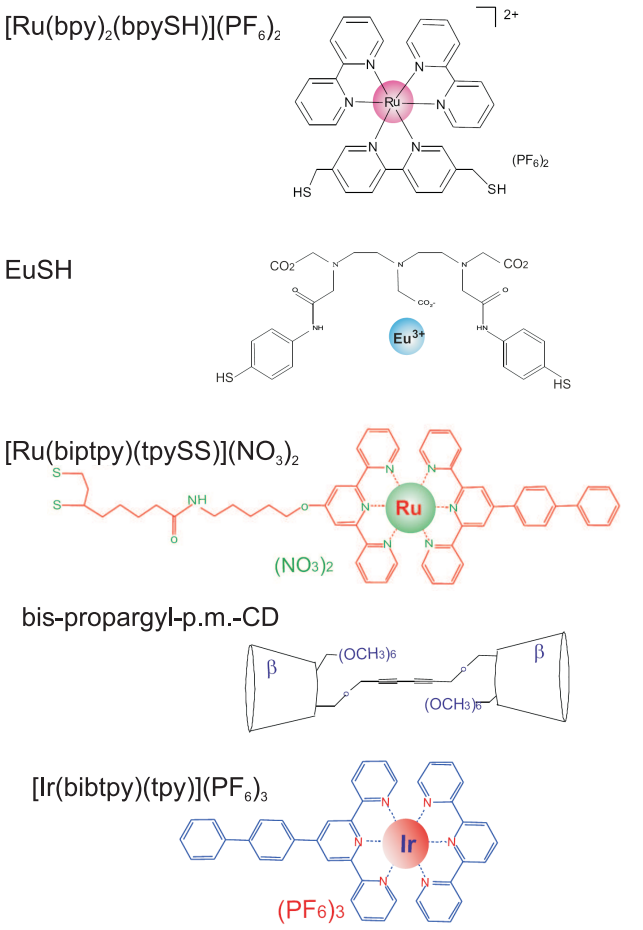

Fig. 2. Chemical structure of the used molecules.

in a solution (10 % CH_3CN in H_2O) of the cyclodextrin unit for two hours and afterwards in a solution (10 % CH_3CN in H_2O) of the iridium complex for two hours. To remove any excess of the cyclodextrin unit and the europium complex, the sample was rinsed with water after both adsorption processes and dried with a gentle flow of nitrogen. In addition, after each drying process, an extinction spectrum has been measured.

III. Results

A. Characterization of the nanoparticles after preparation

The morphological parameters of the nanoparticles have been obtained by AFM and SEM. While SEM reveals the lateral dimensions of the nanoparticles, AFM has been used to determine the hight of the nanoparticles, i.e., the dimension perpendicular to the substrate surface.

The small triangular nanoparticles (cf. figure 1) exhibit a base of the triangle of (74 ± 6) nm, a height of (30 ± 4) nm, and a tip-to-tip distance between two nanoparticles of (102 ± 14) nm. Their optical spectrum is depicted in figure 3. It shows a strong plasmon resonance at $\lambda_{\mathrm{SPR}} = 730$ nm and a less intense resonance at $\lambda_{\mathrm{SPR}} = 550$ nm. The resonances are attributed to the excitation of a dipolar and quadrupolar plasmon resonance, respectively [67, 68].

An AFM image of the large triangular nanoparticles with a base of the triangle of (365 ± 17) nm, a hight of (150 ± 10) nm and a tip-to-tip distance between two nanoparticles of (342 ± 24) nm, is depicted in figure 4. For the simultaneously

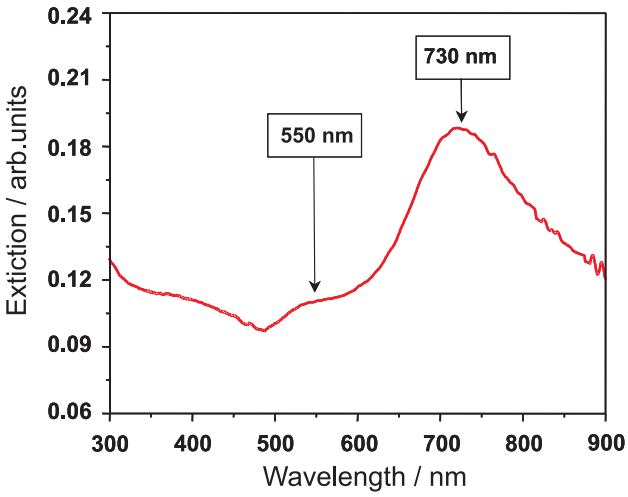

Fig. 3. Extinction spectrum of small triangular gold nanoparticles.

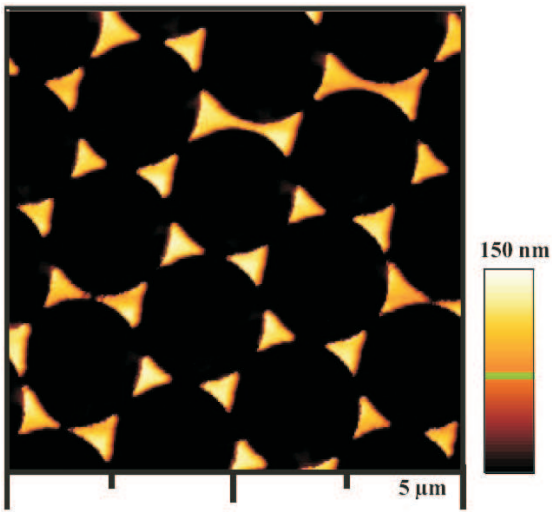

Fig. 4. AFM image of large triangular nanoparticles.

on the same substrate generated large elongated nanoparticles (figure 5) the measurements reveal a length of (365 ± 17) nm, a width of (150 ± 20) nm, a hight of (150 ± 10) nm and a particle-to-particle distance of about $d = (1484 \pm 20)$ nm has been measured.

The extinction spectrum of a sample with both, large triangular and large elongated gold nanoparticles, is depicted in figure 6. Consequently, the spectrum is a superposition of the extinction of the triangular and the elongated nanoparticles. Hence, it exhibits two strong plasmon resonances, one at $\lambda_{SPR} = 730$ nm and one at $\lambda_{SPR} = 650$ nm, attributed to the excitation of the dipolar modes of the two different shaped nanoparticles. The expected absorption band at λ = 550 nm due to the excitation of the quadrupol plasmon resonance of the triangular NPs is super-imposed by the strong absorption band of the elongated particles.

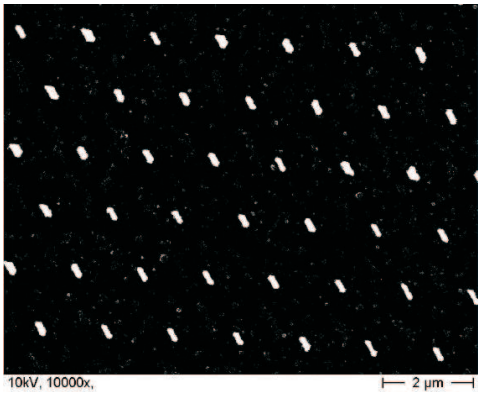

Fig. 5. SEM image of elongated large nanoparticles.

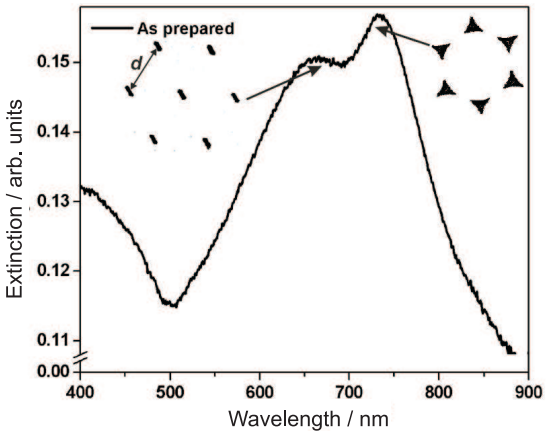

Fig. 6. Extinction spectrum of a substrate with large triangular and large elongated gold nanoparticles.

In addition, confocal microscopy measurements have been performed with large elongated nanoparticles. Figure 7 displays a confocal microscopy image in reflection mode of the nanoparticles. The shape of the nanoparticles as well as their arrangement on the substrate are clearly resolved.

B. Sensitivity measurements

As mentioned previously, for the sensitivity measurements the europium and both ruthenium complexes have been adsorbed on small as well as on large triangular nanoparticles. To strengthen the paper, only the results of the ruthenium complex **1** are explicitly shown. Figure 8a) shows the extinction spectra of small triangular nanoparticles before and after adsorption of the ruthenium complex **1**. An enormous red shift of 61 nm of the dipole resonance due to the adsorption of the molecules is measured. In addition, an absorption peak at 300 nm and an overall increase of the extinction amplitude is observed. While the additional peak at 300 nm is due to a strong absorption band of the molecule in this spectral region, the increased extinction is easily explained by the fact that due to the adsorbed molecules more material contributes to the absorption. Similar experiments have been performed using a sample with large elongated and triangular nanoparticles. Figure 8b) depicts the optical spectra of the sample before and

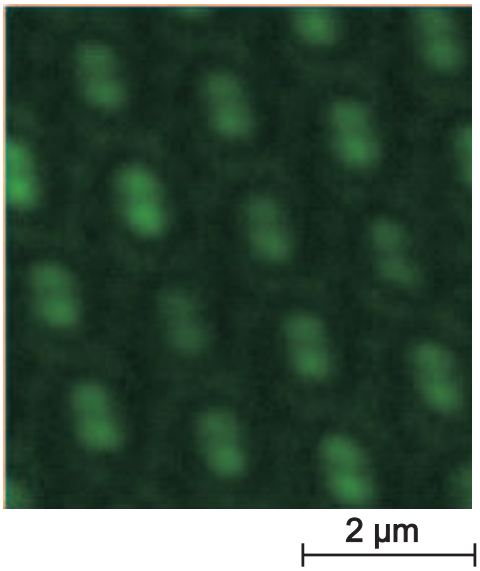

Fig. 7. Confocal microscopy image of large elongated nanoparticles. The image has been obtained in reflection mode.

after adsorption of the ruthenium complex **1**. Since only the dipolar resonance of the triangular nanoparticles can be clearly resolved before and after molecule adsorption, only the shift of this resonance has been evaluated. Here, a red shift of only 14 nm has been measured. In addition, the absorption band of the ruthenium complex **1** at 300 nm and, again, an overall increase of the extinction amplitude has been measured, which can be explained as before.

Similar investigations have been made using the europium complex and the ruthenium complex **2**. Table I summarizes the results obtained with the small triangular nanoparticles. Depending on the adsorbed molecule, we measured red shifts of the dipole plasmon resonance between 20 nm and 61 nm.

TABLE I
MEASURED RED SHIFTS OF THE DIPOLE PLASMON RESONANCE OF SMALL TRIANGULAR NANOPARTICLES FOR DIFFERENT ADSORBED MOLECULES.

Compound	**Solvent**	$\Delta\lambda$ **/ nm**
Ru-complex **1**	Acetonitrile	61 $\pm$ 1 nm
Eu-complex	Methanol	45 $\pm$ 1 nm
Ru-complex **2**	Acetonitrile	20 $\pm$ 1 nm

The plasmon resonance shifts for the large triangular nanoparticles is summarized in table II. For these samples red shifts between 9 nm and 14 nm were measured. Hence, for all investigated molecules a significantly larger plasmon shift and an up to 4 times higher sensitivity is observed for the small triangular nanoparticles. This higher sensitivity of the

TABLE II
MEASURED RED SHIFTS OF THE DIPOLE PLASMON RESONANCE OF LARGE TRIANGULAR NANOPARTICLES FOR DIFFERENT ADSORBED MOLECULES.

Compound	**Solvent**	$\Delta\lambda$ **/ nm**
Ru-complex **1**	Acetonitrile	14 $\pm$ 1 nm
Eu-complex	Methanol	13 $\pm$ 1 nm
Ru-complex **2**	Acetonitrile	9 $\pm$ 1 nm

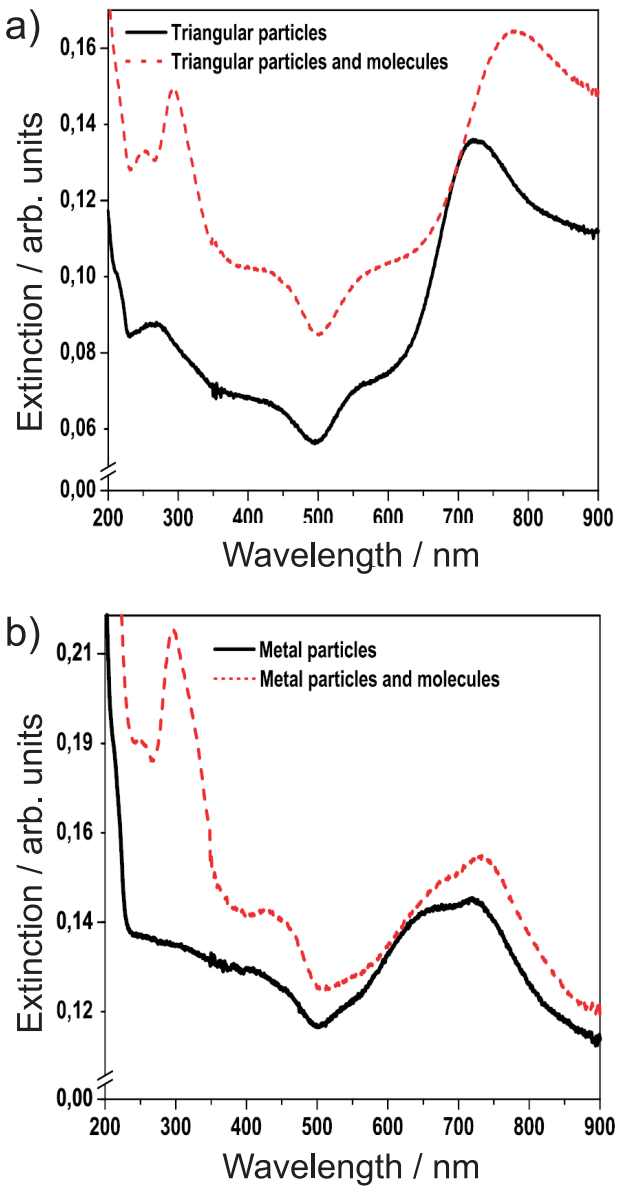

Fig. 8. Extinction spectra of the small triangular nanoparticles (a) and large triangular nanoparticles (b) before and after adsorption of the ruthenium complex 1.

small triangular nanoparticles can be attributed to their higher surface to volume ratio compared to the large triangles.

C. Molecular wire formation

As mentioned previously, confocal microscopy has been applied to prove that the ruthenium complex **2** adsorb only on the gold nanoparticles and not on the substrate. With respect to the limits of resolution of the confocal microscope, only large elongated nanoparticles (cf. figure 5) have been used. Figure 9 depicts the confocal image of a sample with the adsorbed ruthenium complex **2**. The scale of the image is chosen such, that it coincides with the scale in figure 7. The excitation wavelength was $\lambda_{\mathrm{exc}} = 458$ nm and the fluorescence light was detected at $\lambda_{\mathrm{fl}} = 620$ nm. Since the fluorescence pattern have the same arrangement as the nanoparticles on the substrate (cf.

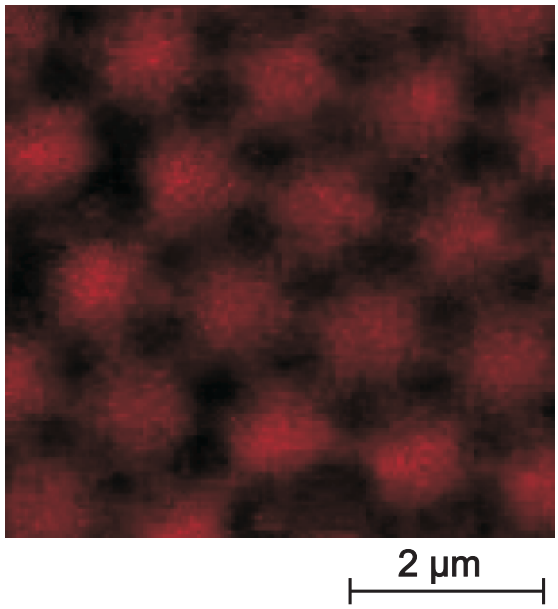

Fig. 9. Confocal microscopy image of the ruthenium complex **2** adsorbed on the gold nanoparticles. The scale is chosen such that it is the same as in figure 7.

figure 7), it is obvious, that the molecules do not attach to the substrate surface. In addition, a large scale confocal image of the ruthenium complex adsorbed on the sample is displayed in figure 10, to demonstrate that the molecule adsorption on the gold nanoparticles is homogeneous over large areas. Hence,

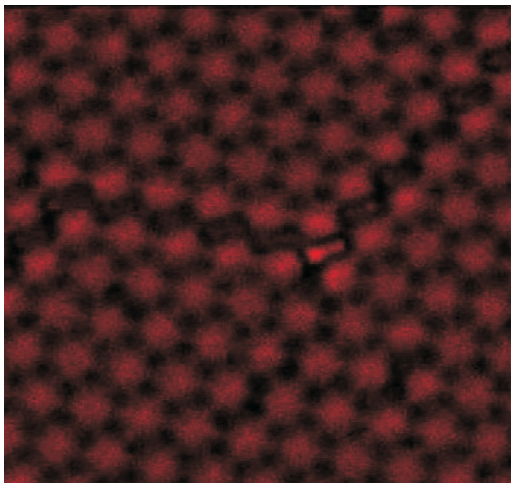

Fig. 10. Large scale confocal microscopy image of the ruthenium complex **2** on the sample.

the ruthenium complex **2** is the ideal start molecule to build a molecular wire on gold nanoparticles.

To monitor the wire formation, again in situ surface plasmon resonance spectroscopy has been applied. Since for the spectroscopy only the shift of the dipolar resonance is relevant, the extinction spectrum is reduced to the corresponding wavelength range. Figure 11 depicts the plasmon resonance of

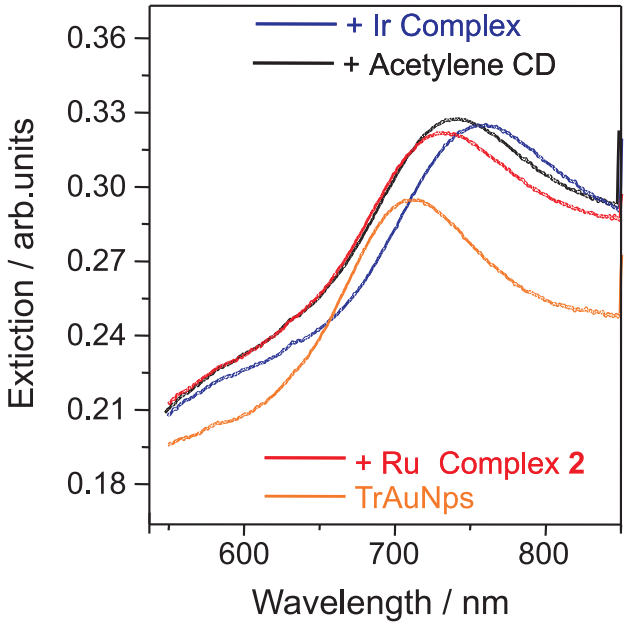

Fig. 11. Extinction spectra of the triangular gold nanoparticles without and with molecules at different stages of wire formation.

TABLE III
PLASMON SHIFTS AS A FUNCTION OF MOLECULAR WIRE LENGTH.

Components	**Resonance** λ **/ nm**	**Total shift** $\Delta\lambda$ **/ nm**
Gold Nanoparticles	713 ± 1	-
Gold Nanoparticles + Ru complex **2**	733 ± 1	20 ± 1
Gold Nanoparticles + Ru complex **2** + cyclodextrins	744 ± 1	31 ± 1
Gold Nanoparticles + Ru complex **2** + cyclodextrins + Ir complex	759 ± 1	46 ± 1

the small triangular gold nanoparticles without and with the stepwise adsorbed molecules. It shows that the adsorption of the ruthenium complex **2** on the gold nanoparticles induces a shift of the plasmon resonance of $\Delta\lambda = 20$ nm. The subsequent binding of the cyclodextrin unit to the ruthenium complex **2** and the binding of the iridium complex to the bound cyclodextrin unit cause additional shifts of $\Delta\lambda = 11$ nm and 15 nm, respectively. Table III summarizes the results. Altogether, the plasmon resonance is shifted by 46 nm due to the wire formation, which demonstrates that in situ surface plasmon resonance is an ideal tool to monitor molecular wire formation on gold nanoparticles.

D. Control experiments

In order to verify that the red shift of the plasmon resonance is due to nanowire formation, control experiments have been accomplished. In a first control experiment, a sample with already formed wires has been immersed in acetonitrile, that breaks the supramolecular bond between the ruthenium complex **2** and the cyclodextrin unit. After immersion an extinction spectrum has been recorded. A back shift of the plasmon resonance to $\lambda = 735$ nm has been measured. This wavelength almost coincides with the position of the plasmon resonance of the triangles before the adsorption of the cyclodextrin unit and the iridium complex, demonstrating a breaking of the wire. In a second control experiment the bare nanoparticles were immersed in a cyclodextrin solution for two hours. After washing and drying of the sample, optical spectroscopy has been performed, but no change of the extinction spectrum occurred. Hence, without the ruthenium complex **2** the cyclodextrin units do not bind on the gold nanoparticles or the substrate. Instead, it is removed by the solvent. Thus, both control experiments clearly demonstrate, that the observed plasmon shift of $\Delta\lambda = 46$ nm is due to molecular wire formation.

IV. CONCLUSIONS

Gold nanoparticle arrays have been prepared by nanosphere lithography and served as anchor points for molecules and molecular wires. To investigate the sensitivity of different sized nanoparticles and to monitor wire formation, in situ surface plasmon resonance spectroscopy has been applied. In a first set of experiments, the sensitivity of different sized triangular nanoparticles has been investigated. We found an up to 4 times higher sensitivity for small triangular nanoparticles upon molecule adsorption, which has been explained by their higher surface to volume ratio compared to large triangles. As a consequence, small triangular nanoparticles have been used as anchor points for molecular wires and to monitor the plasmon shift as a function of wire length. For the molecular wire assembling a ruthenium complex, a cyclodextrin unit, and an iridium complex have been stepwise adsorbed on the gold nanoparticles. We demonstrated that the ruthenium complex induces a plasmon shift of 20 nm. The subsequent adsorption of the cyclodextrin unit and the iridium complex cause additional plasmon shifts of 11 nm and 15 nm, respectively. For the complete wire an plasmon shift of $\Delta\lambda = 46$ nm has been measured. Control experiments showed, that the measured shifts are solely due to nanowire formation on the gold nanoparticles. Consequently, we have demonstrated that in situ surface plasmon resonance spectroscopy is an ideal tool to investigate molecular wire formation on gold nanoparticles.

ACKNOWLEDGMENT

We greatly acknowledge the group of Prof. Dr. Zoe Pikramenou, University of Birmingham for providing the molecules. We acknowledge also the group of Prof. Dr. Thomas Baumert for performing the confocal microscopy measurements. Financial support by the Deutsche Forschungsgemeinschaft and the European Commission under contract number MRTN-CT-2003-504233 is gratefully acknowledged.

REFERENCES

[1] F. Hubenthal, D. Blázquez Sánchez, N. Borg, H. Schmidt, H.-D. Kronfeldt, and F. Träger. Tailor−made metal nanoparticles as SERS substrates. *Appl. Phys. B*, 95:351, 2009.

[2] K. Kneipp, H. Kneipp, I. Itzkan, R.R. Dasari, and M.S. Feld. Surface−enhanced Raman scattering and biophysics. *J. Phys.: Cond. Matt.*, 14:R597, 2002.

[3] P. Zijlstra, J.W.M. Chong, and M. Gu. Five−dimensional optical recording mediated by surface plasmons in gold nanorods. *Nature*, 459:410, 2009.

[4] S. Lal, S.E. Clare, and N.J. Halas. Nanoshell−enabled photothermal cancer therapy: Impending clinical impact. *Acc. Chem. Res.*, 41:1842, 2008.

[5] E. Dickerson, E. Dreaden, X. Huang, I. El-Sayed, H. Chu, S. Pushpanketh, J. McDonald, and M. El-Sayed. Gold nanorod assisted near−infrared plasmonic photothermal therapy (PPTT) of squamous cell carcinoma in mice. *Cancer Lett.*, 269:57, 2008.

[6] S. Ozel and Y.O zel. Nanotechnology in education and general framework of nanomanufacturing. *Intern. J. Educa. Inform. Technol.*, 2:113, 2008.

[7] E.-J. Hong, K.-H. Lee, and W. Wenzel. *Intern. J. Biol. Biomed. Engineering*, 1:46, 2007.

[8] F. Hubenthal. Nanoparticles and their tailoring with laser light. *Eur. J. Phys.*, 30:S49, 2009.

[9] R. Morarescu, L. Englert, B. Kolaric, P. Damman, R.A.L. Vallée, T. Baumert, F. Hubenthal, and F. Träger. Tuning nanopatterns on fused silica substrates: A theoretical and experimental approach. *J. Mater. Chem.*, 21:4076, 2011.

[10] M. Westphalen, U. Kreibig, J. Rostalski, H. Lüth, and D. Meissner. Metal cluster enhanced organic solar cells. *Solar Energy Materials & Solar Cells*, 61:97, 2000.

[11] P. Leiderer, C. Bartels, J. König-Birk, M. Mosbacher, and J. Boneberg. Imaging optical near−fields of nanostructures. *Appl. Phys. Lett*, 85:5370, 2004.

[12] N.N. Nedyalkov, H. Takada, and M. Obara. Nanostructuring of silicon surface by femtosecond laser pulse mediated with enhanced near−field of gold nanoparticles. *Appl. Phys. A*, 85:163, 2006.

[13] A.J. Haes and R.P. Van Duyne. A nanoscale optical biosensor: Sensitivity and selectivity of an approach based on the localized surface plasmon resonance spectroscopy of triangular silver nanoparticles. *J. Am. Chem. Soc.*, 124:10596, 2002.

[14] *http://www.altenberg-dom.de/bilder/53542596a00e70f3a/o000.php*.

[15] *http://www.britishmuseum.org/explore/highlights/highlight_objects/pe_mla/t/the_lycurgus_cup.aspx*.

[16] M. Faraday. The bakerian lecture: Experimental relations of gold (and other metals) to light. *Trans. Roy. Soc. (London)*, 147:145, 1857.

[17] G. Mie. Beiträge zur Optik trüber Medien, speziell kolloidaler Metallösungen. *Annalen der Physik*, 25:377, 1908.

[18] H. Horvath. Gustav Mie and the scattering and absorption of light by particles: Historic developments and basics. *J. Quantum Spectrosc. Radiat. Transfer*, 110:787, 2009.

[19] A. Johari and V. Rana. Investigation of silicon oxide (SiO_x) nanowires growth with gold/chromium catalysts. *Adc. Res. Phys. Eng., Proc. Intern. Conf. Nanotechnol. (Nanotechnology 10, Cambridge UK)*, page 233, 2010.

[20] Z. Chang, S. Li, M. Bouquey, I. Kraus, C.A. Serra, and J.M. Köhler. Continious-microflow synthesis of multiscale materials based on polymer microparticles/inorganic nanoparticles composites. *Adc. Res. Phys. Eng., Proc. Intern. Conf. Nanotechnol. (Nanotechnology 10, Cambridge UK)*, page 135, 2010.

[21] W. Benten, N. Nilius, N. Ernst, and H.-J. Freund. Photon emission spectroscopy of single oxide−supported Ag−Au alloy clusters. *Phys. Rev. B*, 72:045403, 2005.

[22] C. Sönnichsen, T. Franzl, T. Wilk, G. von Plessen, J. Feldmann, O. Wilson, and P. Mulvaney. Drastic reduction of plasmon damping in gold nanorods. *Phys. Rev. Lett.*, 88:077402, 2002.

[23] S. Berciaud, L. Cognet, P. Tamarat, and B. Lounis. Observation of intrinsic size effects in the optical response of individual gold nanoparticles. *Nano Lett.*, 5:515, 2005.

[24] O.L. Muskens, D. Christofilos, N. Del Fatti, and F. Vallée. Optical response of a single noble metal nanoparticle. *J. Opt. A: Pure Appl. Opt.*, 8:S264, 2006.

[25] O.L. Muskens, G. Bachelier, N. Del Fatti, F. Vallée, A. Brioude, X. Jiang, and M.-P. Pileni. Quantitative absorption spectroscopy of a single gold nanorod. *J. Phys. Chem. C*, 112:8917, 2008.

[26] N. Del Fatti, D. Christofilos, and F. Vallée. Optical response of a single gold nanoparticle. *Gold Bull.*, 41/2:147, 2008.

[27] C. Novo, D. Gomez, J. Perez-Juste, Z. Zhang, H. Petrova, M. Reismann, P. Mulvaney, and G.V. Hartland. *Phys. Chem. Chem. Phys.*, 8:3540, 2006.

[28] M. Hu, C. Novo, A. Funston, H. Wang, H. Staleva, S. Zouc, P. Mulvaney, Y. Xiae, and G.V. Hartland. Dark-field microscopy studies of single metal nanoparticles: understanding the factors that influence the linewidth of the localized surface plasmon resonance. *J Mater Chem.*, 18:1949, 2008.

[29] T. Ziegler, C. Hendrich, F. Hubenthal, T. Vartanyan, and F. Träger. Dephasing times of surface plasmon excitation in Au nanoparticles determined by persistent hole burning. *Chem. Phys. Lett.*, 386:319, 2004.

[30] H. Ouacha, C. Hendrich, F. Hubenthal, and F. Träger. Laser−assisted growth of gold nanoparticles: Shaping and optical characterization. *Appl. Phys. B*, 81:663, 2005.

[31] F. Hubenthal, T. Ziegler, C. Hendrich, M. Alschinger, and F. Träger. Tuning the surface plasmon resonance by preparation of gold−core/silver−shell and alloy nanoparticles. *Eur. Phys. J. D*, 34:165, 2005.

[32] F. Hubenthal, C. Hendrich, H. Ouacha, D. Blázquez Sánchez, and F. Träger. Preparation of gold nanoparticles with narrow size distribution and well defined shapes. *Int. J. Mod. Phys. B*, 19:2604, 2005.

[33] P.K. Jain, K.S. Lee, I.H. El-Sayed, and M.A. El-Sayed. Calculated absorption and scattering properties of gold nanoparticles of different size, shape, and composition: Applications in biological imaging and biomedicine. *J. Phys. Chem.*, 110:7238, 2006.

[34] V. Myroshnychenko, J. Rodríguez-Fernández, I. Pastoriza-Santos, A.M. Funston, C. Novoc, P. Mulvaney, L.M. Liz-Marzán, and F.J. García de Abajo. Modelling the optical response of gold nanoparticles. *Chem. Soc. Rev.*, 37:1792, 2008.

[35] O.L. Muskens, P. Billaud, M. Broyer, N. Del Fatti, and F. Vallée. Optical extinction spectrum of a single gold nanoparticle: Quantitative characterization of a particle and its local environment. *Phys. Rev. B*, 78:205410, 2008.

[36] H. Baida, P. Billaud, S. Marhaba, D. Christofilos, E. Cottancin, A. Crut, J. Lermé, P. Maioli, M. Pellarin, M. Broyer, N. del Fatti, F. Vallée, A. Sánchez-Iglesias, I. Pastoriza-Santos, and L.M. Liz-Marzán. Quantitative determination of the size dependence of surface plasmon resonance damping in single ag at sio_2 nanoparticles. *Nano Lett.*, 9:3463, 2009.

[37] F. Hubenthal, C. Hendrich, and F. Träger. Damping of the localized surface plasmon polariton resonance of gold nanoparticles. *Appl. Phys. B*, 100:225, 2010.

[38] E. Le Ru, J. Grand, N. Felidj, J. Aubard, G. Levi, A. Hohenau, J.R. Krenn, E. Blackie, and P. Etchegoin. Experimental verification of the SERS electromagnetic model beyond the $|E|^4$ approximation: Polarization effects. *J. Phys. Chem.*, 112:8117, 2008.

[39] A. Otto. What is observed in single molecule SERS, and why? *J. Raman Spectrosc.*, 33:593, 2002.

[40] W.E. Doering and S. Nie. Single−molecule and single−nanoparticle SERS: Examining the roles of surface active sites and chemical enhancement. *J. Phys. Chem. B*, 106:311, 2002.

[41] S. Lucht, T. Murphy, H. Schmidt, and H.-D. Kronfeldt. Optimized recipe for solgel−based SERS substrates. *J. Raman Spectrosc.*, 31:1017, 2000.

[42] H. Schmidt, K. Sowoidnich, and H.-D. Kronfeldt. A prototype handheld raman sensor for the in-situ characterization of meat quality. *Appl. Spectr.*, 64:888, 2010.

[43] M. Maiwald, H. Schmidt, B. Sumpf, R. Güther, G. Erbert, H.-D. Kronfeldt, and G. Tränkle. Microsystem light source at 488 nm for shifted excitation resonance raman difference spectroscopy. *Appl. Spectr.*, 63:1283, 2009.

[44] H. Grebel. Surface-enhanced raman scattering: phenomenological approach. *J. Opt. Soc. Am. B*, 21:429, 2004.

[45] J. Krenn. Nanoparticle waveguides: Watching energy transfer. *Nature Materials*, 2:210, 2003.

[46] A.B. Evlyukhin, C. Reinhardt, E. Evlyukhina, and B.N. Chichkov. Asymmetric and symmetric local surface−plasmon−polariton excitation on chains of nanoparticles. *Optics Lett.*, 34:2237, 2009.

[47] J. Lakowicz, B. Shen, S. D'Auria, J. Malicka, J. Fang, Z. Gryczynski, and I. Gryczynski. Radiative decay engineering 2. Effects of silver island films on fluorescence intensity, lifetimes, and resonance energy transfer. *Analytical Biochem.*, 301:261, 2002.

[48] A. Bek, R. Jansen, M. Ringler, S. Mayilo, T.A. Klar, and J. Feldmann. Fluorescence enhancement in hot spots of AFM−designed gold nanoparticle sandwiches. *Nano Lett.*, 8:485, 2008.

[49] I. Gryczynski, J. Malicka, Y. Shen, Z. Gryczynski, and J. Lakowicz. Multiphoton excitation of fluorescence near metallic particles: Enhanced and localized excitation. *J. Phys. Chem. B*, 106:2191, 2002.

[50] M. Alschinger, M. Maniak, F. Stietz, T. Vartanyan, and F. Träger. Application of metal nanoparticles in confocal laser scanning microscopy:

improved resolution by optical field enhancement. *Appl. Phys. B*, 76:771, 2003.

[51] J. Boneberg, J. König-Birk, H.-J. Münzer, P. Leiderer, K.L. Shuford, and G.C. Schatz. Optical near−fields of triangular nanostructures. *Appl. Phys. A*, 89:299, 2007.

[52] N. Nedyalkov, T. Sakai, T. Miyanishi, and M. Obara. Near field distribution in two dimensionally arrayed gold nanoparticles on platinum substrate. *Appl. Phys. Lett.*, 90:123106, 2007.

[53] S.D. Berger, J.M. Gibson, R.M. Camarda, R.C. Farrow, H.A. Huggins, J.S. Kraus, and J.A. Liddle. Projection electron−beam lithography: A new approach. *J. Vac. Sci. Technol. B*, 9:2996, 1991.

[54] H.G. Rubahn. *Nanophysik und Nanotechnologie*. Teubner Verlag, Wiesbaden, 2004.

[55] F. Hubenthal. *Noble Metal Nanoparticles: Synthesis and Optical Properties. In: Andrews DL, Scholes, GD and Wiederrecht GP (eds.) Comprehensive Nanoscience and Technology, volume 1, pp. 375435*. Oxford: Academic Press, 2010.

[56] B. Wu and A. Kumar. Extreme ultraviolet lithography: A review. *J. Vac. Sci. Technol. B*, 25:1743, 2007.

[57] J.M. Kontio, H. Husu, J. Simonen, M.J. Huttunen, J.Tommila, M. Pessa, and M. Kauranen. Nanoimprint fabrication of gold nanocones with 10 nm tips for enhanced optical interactions. *Optics Lett.*, 34:1979, 2009.

[58] U.C. Fischer and H.P. Zingsheim. Submicroscopic pattern replication with visible light. *J. Vac. Sci. Technol.*, 19:881, 1981.

[59] R. Morarescu, D. Blázquez Sánchez, N. Borg, T. Vartanyan, F. Träger, and F. Hubenthal. Shape tailoring of hexagonally ordered triangular gold nanoparticles with nanosecond−pulsed laser light. *Appl. Surf. Sci.*, 225:9822, 2009.

[60] F. Hubenthal, R. Morarescu, L. Englert, L. Haag, T. Baumert, and F. Träger. Parallel generation of nanochannels in fused silica with a single femtosecond laser pulse: Exploiting the optical near fields of triangular nanoparticles. *Appl. Phys. Lett.*, 95:063101, 2009.

[61] X.D. Wang, E. Graugnard, J.S. King, Z.L. Wang, and C.J. Summers. Large−scale fabrication of ordered nanobowl arrays. *Nano Lett.*, 4:2223, 2004.

[62] C.L. Haynes, A.D. McFarland, M.T. Smith, J.C. Hulteen, and R.P. Van Duyne. Angle−resolved nanosphere lithography: Manipulation of nanoparticle size, shape, and interparticle spacing. *J. Phys. Chem. B*, 106:1898, 2002.

[63] J.C. Hulteen, D.A. Treichel, M.T. Smith, M.L. Duval, T.R. Jensen, and R.P. Van Duyne. Nanosphere lithography: Size−tunable silver nanoparticle and surface cluster arrays. *J. Phys. Chem. B*, 103:3854, 1999.

[64] F. Sun, W. Cai, Y. Li, G. Duan, W.T. Nichols, C. Liang, N. Koshizaki, Q. Fang, and I.W. Boyd. Laser morphological manipulation of gold nanoparticles periodically arranged on solid supports. *Appl. Phys. B*, 81:765, 2005.

[65] R. Micheletto, H. Fukuda, and M. Ohtsu. A simple method for the production of a two−dimensional, ordered array of small latex particles. *Langmuir*, 11:3333, 1995.

[66] R. Morarescu. Preparation and applications of periodical gold nanoparticle arrays. *PhD Thesis, University of Kassel*, 2009.

[67] K.L. Shuford, M.A. Ratner, and G.C. Schatz. Multipolar excitation in triangular nanoprisms. *J. Chem. Phys.*, 123:114713, 2005.

[68] J.E. Millstone, S. Park, K.L. Shuford, L. Qin, G.C. Schatz, and C.A. Mirkin. Observation of a quadrupole plasmon mode for a colloidal solution of gold nanoprisms. *J. Am. Chem. Soc.*, 127:5312, 2005.